PAPER • OPEN ACCESS

The detention performance enhancement of single gallium arsenide nanowire photodetector by nitrogen plasma treatment

To cite this article: Hao Huang *et al* 2025 *Nanotechnology* **36** 255202

View the article online for updates and enhancements.

The detention performance enhancement of single gallium arsenide nanowire photodetector by nitrogen plasma treatment

Hao Huang[1,2,3,4,*] , Dong Xu[1,5,6] , Tao Li[2,3], Renda Gui[4], Shuo Li[7] , Wai-Hung Ip[8] and Kai-Leung Yung[8]

[1] Taizhou Key Laboratory of Minimally Invasive Interventional Therapy & Artificial Intelligence, Taizhou Campus of Zhejiang Cancer Hospital (Taizhou Cancer Hospital), Taizhou 317502, People's Republic of China
[2] College of Computer Science, Nankai University, Tianjin 300350, People's Republic of China
[3] Xingchuang Haihe Laboratory, Tianjin 300350, People's Republic of China
[4] Hubei Key Laboratory of Micro-Nanoelectronic Materials and Devices, Key Laboratory of Intelligent Sensing System and Security of the Ministry of Education, School of Microelectronics, Hubei University, Wuhan 430062, People's Republic of China
[5] Department of Diagnostic Ultrasound Imaging & Interventional Therapy, Zhejiang Cancer Hospital, Hangzhou Institute of Medicine (HIM), Chinese Academy of Sciences, Hangzhou 310022, People's Republic of China
[6] Wenling Institute of Big Data and Artificial Intelligence in Medicine, Taizhou 317502, People's Republic of China
[7] Department of Clinical Laboratory, Institute of Translational Medicine, Renmin Hospital of Wuhan University, Wuhan 430060, People's Republic of China
[8] Department of Industrial and Systems Engineering, The Hong Kong Polytechnic University, Hong Kong Special Administrative Region of China, 100872, People's Republic of China

E-mail: haohuang@hubu.edu.cn

CrossMark

Abstract

Sensors based on gallium arsenide (GaAs) nanowires (NWs) have excellent sensitivity and can directly detect individual virus particles and individual DNA molecules. GaAs NW photodetectors have attracted wildly attentions due to their direct band gap, specific surface area and high optical absorption coefficient. However, GaAs NWs suffer the problem of serious surface states, leading to the development of high performance GaAs NW photodetectors. Plasma treatment with inert gas is one of the important methods to reduce the density of surface states. In this paper, the effect of nitrogen plasma treatment on the performance of GaAs NW photodetector is investigated. The results show that the light current of GaAs NW photodetector

---

is obviously increased. Besides, the responsivity, specific detectivity and external quantum efficiency (EQE) are also improved. Under 808 nm laser with the light intensity is 2966.8 mW cm^{-2}, the responsivity changes from 56.4 A W^{-1} to 117.6 A W^{-1} and 18.7 A W^{-1}, the specific detectivity changes from 4.7×10^{11} Jones to 9.9×10^{11} Jones and 3.2×10^{11} Jones, the EQE changes from 13 146% to 27 434% and 4359% when the nitrogen plasma treatment time is 0 s, 10 s and 20 s, respectively. This may be related to the defect states density of NWs is changed after nitrogen plasma treatment. This work promotes the further development of GaAs NW photodetectors for biosensing techniques.

Supplementary material for this article is available online

Keywords: biosensor, gallium arsenide, nanowires, photodetector, plasma treatment

1. Introduction

One dimensional (1D) semiconductor nanowires (NWs) have the advantages of small size, large specific surface area, high carrier mobility, and tunable light absorption, thus NWs usually exhibit excellent optoelectronic properties, such as ultrahigh optoelectronic gain, multi array light limiting effect, and sub-wavelength size effect, and can be applied in optical imaging and sensing, environmental monitoring, chemical/biological sensing, and rocket plume detection [1–6]. To date, NWs have been widely used in interconnect systems as well as electronic and optoelectronic functional devices. Semiconductor NWs have shown many potential applications in medical and biological detection fields due to their unique electrical, optical, and chemical properties. Sensors based on NWs have excellent sensitivity and can directly detect individual virus particles and individual DNA molecules [7, 8]. The biosensor utilizing ZnO NWs exhibits a high sensitivity for detecting glucose concentrations within the range of 0.1–100 mM [9, 10]. Sensing devices based on NWs have been employed to monitor concentrations of uric acid and urea in blood samples, providing valuable insights into the assessment of conditions such as gout (a form of arthritis) and kidney disease [11, 12]. Optical sensors based on NWs have been proven to be suitable for the evanescent field of NWs waveguides, [13] NWs based LEDs have been proven to be suitable as room temperature single photon sources, [14] the coaxial NWs structure has shown special prospects in the field of solar cells [15].

In the past decade, with the development of semiconductor processing technology, photodetectors based on 1D NWs and two-dimensional materials have become a research hotspot. As a typical III–V semiconductor, gallium arsenide (GaAs) has a direct bandgap of 1.42 eV, which located in near-infrared band, besides, GaAs shows high electron mobility, high saturation drift rate, small dielectric constant, and high temperature resistance, which make it shows great potential for applications in the preparation of room temperature electronic and optoelectronic devices [16–20]. With the development of portable devices, it is imperative to shrink bulk materials to the nanoscale. However, when GaAs is reduced to 1D GaAs NWs, surface current will be generated owing to the high surface

state density of GaAs NWs, resulting in an increase in dark current and a decrease in photocurrent. This is detrimental to the implementation of high-performance GaAs based NWs photodetectors. Finally, it is essential to highlight that the possibility of achieving extremely high doping in GaAs NWs, facilitated by the unique characteristics of GaAs, opens the avenue for using these NWs not only in low-temperature microscopic physics experiments but also in modern nanoscale devices [21]. This breakthrough in understanding GaAs properties not only enhances its applicability in the field of low-temperature mesoscopic physics but also removes obstacles for its potential application in the realm of biosensing.

Passivation the surface state of NWs is an important strategy to improve the performance of GaAs NW photodetectors. Sulfur solution passivation methods, such as Na$_2$S, (NH$_4$)$_2$S, etc, are widely used in III–V semiconductor materials and devices, which can effectively remove the surface oxide layer and dangling bonds, simultaneously generate new stable chemical bonds on the surface [22–24]. The effects of sulfur solution passivation on optical and electrical properties of GaAs NWs have also been extensively studied [25–27]. The photoluminescence (PL) intensity and conductivity of GaAs NWs will increase. Recent report has studied the effect of sulfur solution passivation on the optoelectronic properties of GaAs NWs photodetector, where the dark current is reduced and the photocurrent is improved after sulfur passivation [28]. The effect of nitrogen solution passivation (N$_2$H$_4 \bullet$H$_2$O) on the electrical and optoelectronic properties of GaAs NWs have been also studied, where the electrical conductivity of NWs is enhanced and the PL intensity is enhanced after passivation. The improved performance is mainly due to the decrease of the surface state density of NWs after nitrogen passivation [25]. Although passivation of GaAs NWs by solution methods has been studied, the solution method is not environmentally friendly. Thus, reducing the surface states density of GaAs NWs by dry passivation should be explored, such as growth of protective layer, [29–31] and plasma treatment [32–34]. The GaAs NWs have been passivated by Al$_x$Ga$_{1−x}$As shell, where the minority carrier diffusion length increases, the PL lifetime and intensity also increase [30]. The optical performance of GaAs NWs has been improved by mixed nitrogen–hydrogen

plasma treatment, after treatment, the surface states are passivated, and the rate of nonradiative recombination is reduced [33]. However, the effect of plasma treatment on the optoelectronic properties of GaAs NWs need to be further studied.

Here, we synthesized GaAs NWs through a chemical vapor deposition (CVD) method. Then the GaAs NWs were fabricated into single GaAs NW photodetector. The optoelectronic properties of the single GaAs NW photodetector before and after nitrogen plasma treatment were studied by a Agilent 4155C semiconductor analyzer under a 808 nm laser. The single GaAs NW device exhibit P-type semiconductor behavior. After nitrogen plasma treatment, the hysteresis of the device is reduced. Besides, the light currents of the single GaAs NW photodetector increases after nitrogen plasma treatment, which change from 25.9 nA to 78.3 nA and 41.8 nA when the treatment time is 0 s, 10 s and 20 s, the treatment power is 10 W, and the light intensity is 2966.8 mW cm^{-2}. Simultaneously, the responsivity, external quantum efficiency (EQE) and specific detectivity also enhance after nitrogen plasma treatment. When the light intensity is 0.3 mW cm^{-2}, the responsivity changes from 56.4 A W^{-1} to 117.6 A W^{-1} and 18.7 A W^{-1}, the EQE changes from 13 146% to 27 434% and 4359%, the specific detectivity changes from 4.7×10^{11} Jones to 9.9×10^{11} Jones and 3.2×10^{11} Jones. When the light intensity is 2966.8 mW cm^{-2}, the responsivity changes from 1.2 A W^{-1} to 3.5 A W^{-1} and 1.9 A W^{-1}, the EQE changes from 270% to 821% and 438%, the specific detectivity changes from 1.1×10^{9} Jones to 1.9×10^{9} Jones and 1.4×10^{9} Jones. The response time of the single GaAs NW photodetector were also studied. The photocurrent rise time change from 8.32 ms to 4.48 ms and 37.76 ms, the photocurrent fall time change from 52.48 ms to 68.8 ms and 45.78 ms. The change in the optoelectronic properties of the device may be related to the change in the defect states before and after nitrogen plasma treatment. This work is significant for realizing high performance GaAs-based NWs photodetectors and will promote their further applications in civilian and military.

2. Methods

The GaAs NWs are synthesized in a CVD system. The substrate used here is Si with 300 nm SiO_2. Before the NWs were synthesized, 2 nm Au was evaporated on the substrate followed by annealing at 700 °C for 15 min at nitrogen atmosphere. The 2 nm Au was used as catalysts. The GaAs powders (~1 g, 99.9999% purity) were placed into a boron nitride crucible and then the crucible was placed at the center of two-zone tube furnace. The prepared substrate was placed on the other crucible, and the crucible with substrate was placed at the downstream zones of the crucible with GaAs powders, with a position of 5 cm. During the synthesis process, the vacuum of the CVD system was maintained at 5×10^{-2} Pa, the carrier gases were H_2, the flow rate were 100 SCCM, the synthesis time was 1 h, the synthesis temperature was 900 °C. After the synthesis process, the temperature was cooled down to room

temperature naturally at H_2 atmosphere. The GaAs NWs were obtained.

The synthesized GaAs NWs was fabricated into single GaAs NWs photodetector. The GaAs NWs were transferred onto Si substrate with the SiO_2 of 300 nm by physical method, i.e. the as-synthesized NWs are directly contacted with the substrate with 300 nm SiO_2, and some NWs are adsorbed on the substrate by using the intermolecular force. Nitrogen was used to blow away the unstable NWs. The MMA/PMMA were spin coated onto the substrate surface and covered the GaAs NWs. Electron beam lithography was used to pattern the designed electrodes. The sample coated with photoresist is introduced into the electron beam lithography machine, and the electrode pattern is drawn by CAD. After that, the pattern is exposed by electron beam lithography machine according to the electrode pattern, and the sample is taken out after exposure, and the electrode shape is exposed in the developer. Then the samples were immersed in HF solution (2%) for 20 s to remove the natural oxide layer on the surface of GaAs NW, after removing the natural oxide layer, the samples are immediately evaporated for 15 nm Cr/50 nm Au as electrodes in a vacuum thermal evaporation coating machine. A single GaAs NW photodetector was prepared by stripping excess metal from acetone.

The electrical and optoelectronic properties were studied by Agilent 4155C semiconductor analyzer with a probe station at vacuum. Nitrogen plasma treatment was performed by plasma cleaner. In plasma treatment process, keep the mechanical pump open while 99.9% nitrogen is fed into the plasma cleaner, the vacuum of the plasma cleaner is kept as 10 Pa, and the power is 10 W. A laser with the wavelength of 808 nm was used to measure the optoelectronic properties of the device.

3. Results

The scanning electron microscope (SEM) image of the as-synthesized GaAs NWs was performed in figure 1. NWs and microwires can be seen in the SEM. The diameters of NWs are about 100 nm, with the lengths of 2–30 μm. The diameters of microwires are about 2–5 μm, with the lengths of 20–80 μm. Besides, the number of NWs is obviously more than the number of microwires. Low-temperature PL of the as-synthesized GaAs NWs before and after nitrogen plasma treatment under 77 K, with the excitation wavelength of 447 nm. The results are shown in figure S1. The PL spectra of the NWs did not show any significant changes in shape before and after nitrogen plasma treatment, but the peak wavelength shifted to shorter wavelength after nitrogen plasma treatment. Besides, the full width at half maximum tends to narrow, which may be due to the reduction of defects after nitrogen plasma treatment.

The NWs were picked out to fabricated single GaAs NW photodetector. The schematic diagram of the single GaAs NW photodetector is shown figure 2(a). A 300 nm SiO_2 is arranged on the high-conductive silicon substrate, GaAs NW is placed on the SiO_2 layer, and the two ends of the NW are covered with

(a)   **(b)**
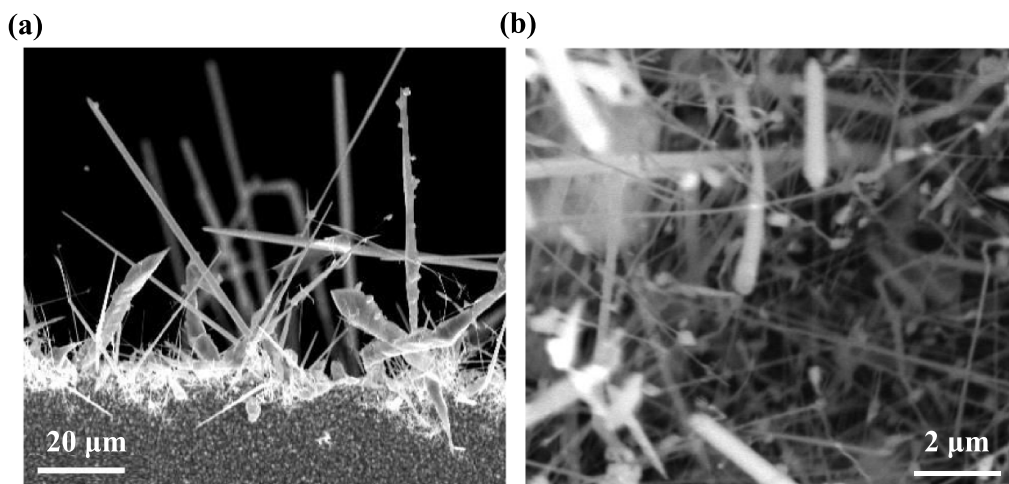
Figure 1. (a) Cross-sectional SEM image of as-synthesized GaAs NWs, scale bar: 20 μm; (b) top-view SEM image of as-synthesized GaAs NWs, scale bar: 2 μm.
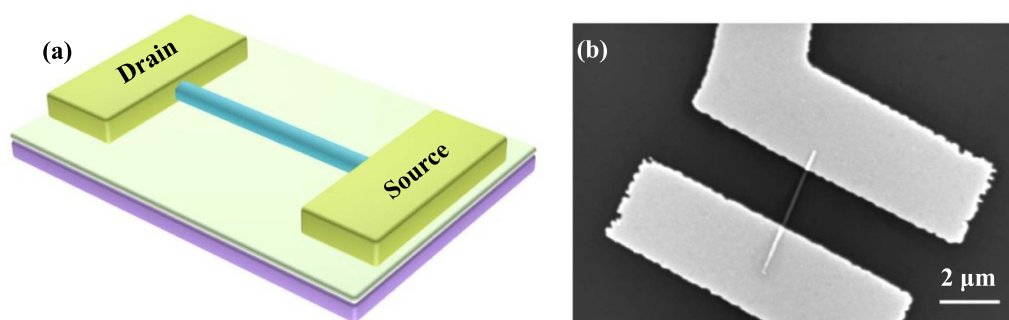
Figure 2. (a) Schematic diagram of the single GaAs NW photodetector; (b) SEM image of the single GaAs NW photodetector, scale bar: 2 μm.

two metal electrodes. The high-conductive silicon substrate is worked as back-gate, the 300 nm SiO_2 is worked as gate dielectric, the GaAs NW is worker as photosensitive material, the two metal electrodes are worked as drain and source. The SEM image of the single GaAs NW photodetector is shown in figure 2(b), with the channel length of 2 μm.

The electrical and optoelectronic properties of the single GaAs NW photodetector before and after nitrogen plasma treatment were studied by Agilent 4155C semiconductor analyzer at vacuum. The nitrogen plasma treatment was performed by plasma cleaner. The treatment power is 10 W, the treatment times are 10 s and 20 s. Figure 3 shows the transfer properties of the single GaAs NW before and after nitrogen plasma treatment. The current of the all the single GaAs NW before and after nitrogen plasma GaAs NW field-effect transistors (FETs) decrease with increasing the gate voltages, indicating that the GaAs NW FETs exhibits p-type semiconductor behavior [28, 35], which may be related to Ga vacancies formed during the synthesis process [36]. All the single GaAs NW before and after nitrogen plasma treatment show significant hysteresis windows. The hysteresis window of the original GaAs NW is $\sim$70 V, after nitrogen plasma treatment for 10 s, the hysteresis window changes to $\sim$50 V, increase the treatment time to 20 s, the hysteresis window changes to

$\sim$60 V. Besides, the threshold shifts to positive direction after treatment for 10 s, and will shift to negative direction. The change in hysteresis window and threshold may be related to the change in defect of the GaAs NW after nitrogen plasma treatment [33].

The optoelectronic properties of the single GaAs NW photodetector before and after nitrogen plasma treatment under different light power intensities are shown in figure 4. As shown in figure 4(a), original GaAs NW photodetector shows obvious photoresponse under 808 nm illumination. With the light power intensity increases from 0.3 mW cm^{-2} to 2966.8 mW cm^{-2}, the light current increases gradually. After nitrogen plasma treatment for 10 s, as shown in figure 4(b), the light currents becomes larger, which means that the single GaAs NW photodetector after nitrogen plasma shows better photoresponse than that of the original device. Increasing the treatment time to 20 s, which is shown in figure 4(c), the light current changes to smaller than the light current when the treatment time is 10 s. When the light intensity is 2966.8 mW cm^{-2}, the light currents of the single GaAs NW photodetector before and after nitrogen plasma are 25.9 nA, 78.3 nA, and 41.8 nA, respectively. Nitrogen plasma treatment has improved the light current of GaAs NW photodetector. To verify the changes in the current after N2 plasma treatment
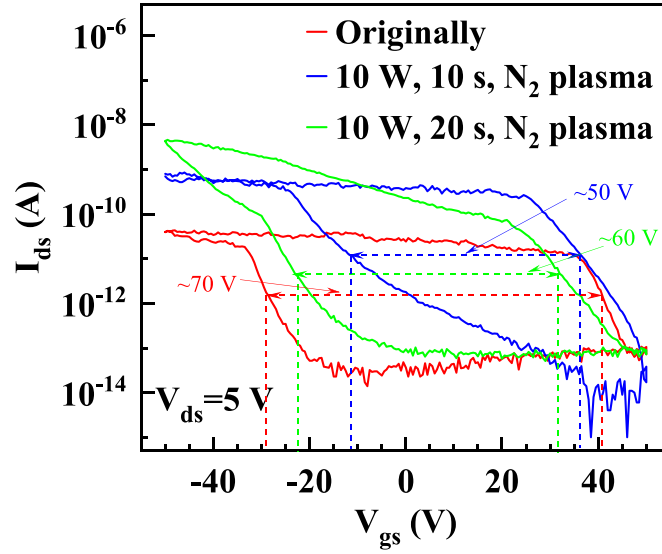
Figure 3. Transfer properties of the single GaAs NW device before and after nitrogen plasma treatment.
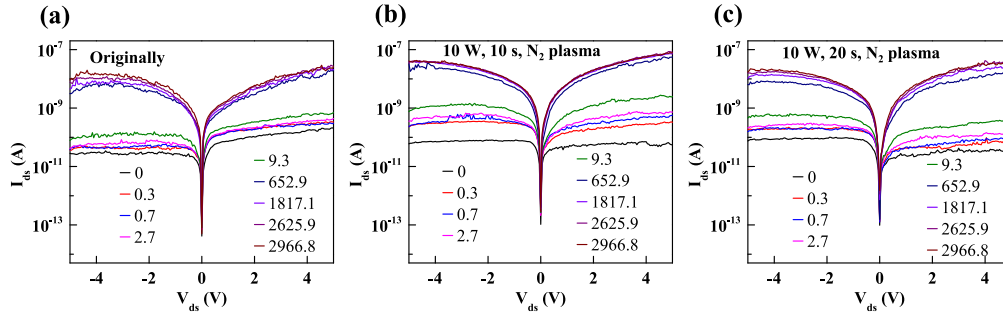
Figure 4. (a) Optoelectronic properties of the original single GaAs NW photodetector; (b) optoelectronic properties of the single GaAs NW photodetector after nitrogen plasma treatment for 10 s; (c) optoelectronic properties of the single GaAs NW photodetector after nitrogen plasma treatment for 20 s; the laser wavelength is 808 nm, with the light power intensity range from 0.3 mW cm^{-2} to 2966.8 mW cm^{-2}.

are reliable, we have measured the *I–V* curves from another device, as shown in figure S2. It shows similar phenomenon compared with the previous *I–V* curves. Thus the results are reliable.

The dependence between light current and power intensity of the single GaAs NW photodetector after nitrogen plasma treatment are shown in figure 5(a). Power law, $I \propto P^k$, can be used to fit the dependence between light current and power intensity, where *I* is the light current, *P* is the light power intensity. *k* is related to the defects of the materials. A larger *k* means the less the defects in the materials [37, 38]. It can be seen that the *k* of the single GaAs NW photodetector after nitrogen plasma treatment is 0.51, 0.63, and 0.73, respectively. The results show that *k* becomes larger after nitrogen plasma treatment. It means the nitrogen plasma treatment have reduced the defect of GaAs NWs. The change trend of hysteresis windows and *k* values seems different, which may be related to the change in interface properties. Nitrogen plasma treatments have reduced the defect of GaAs NWs, leading to the increased *k* and decreased hysteresis windows. However, when the treatment time is long, the nitrogen plasma may change the quality of SiO$_2$, leading to the interface property

between GaAs NW and SiO$_2$ changes, thus the hysteresis window becomes larger.

Responsivity (*R*), EQE and specific detectivity (D^*) are important parameters to evaluate the performance of photodetectors. Responsivity, defined as the ratio of photocurrent to incident light power, characterizes the photodetector's ability to convert optical radiation signals into electrical signals, and can be expressed as follows [39–42]:

$$R = \frac{I_{\text{light}} - I_{\text{dark}}}{A \times P} \quad (1)$$

where I_{light} is the light current, I_{dark} is the dark current, *P* is the light power intensity, *A* is the device area, which is defined as the product of channel length and width, i.e., $A = 2\ \mu\text{m} \times 100\ \text{nm} = 0.2\ \mu\text{m}^2$.

EQE is defined as the ratio of the number of charge carriers collected to the number of incident photons irradiated on the device. EQE can be described as follows [35, 43]:

$$\text{EQE} = \frac{\text{hc}}{\text{e}\lambda}R \quad (2)$$
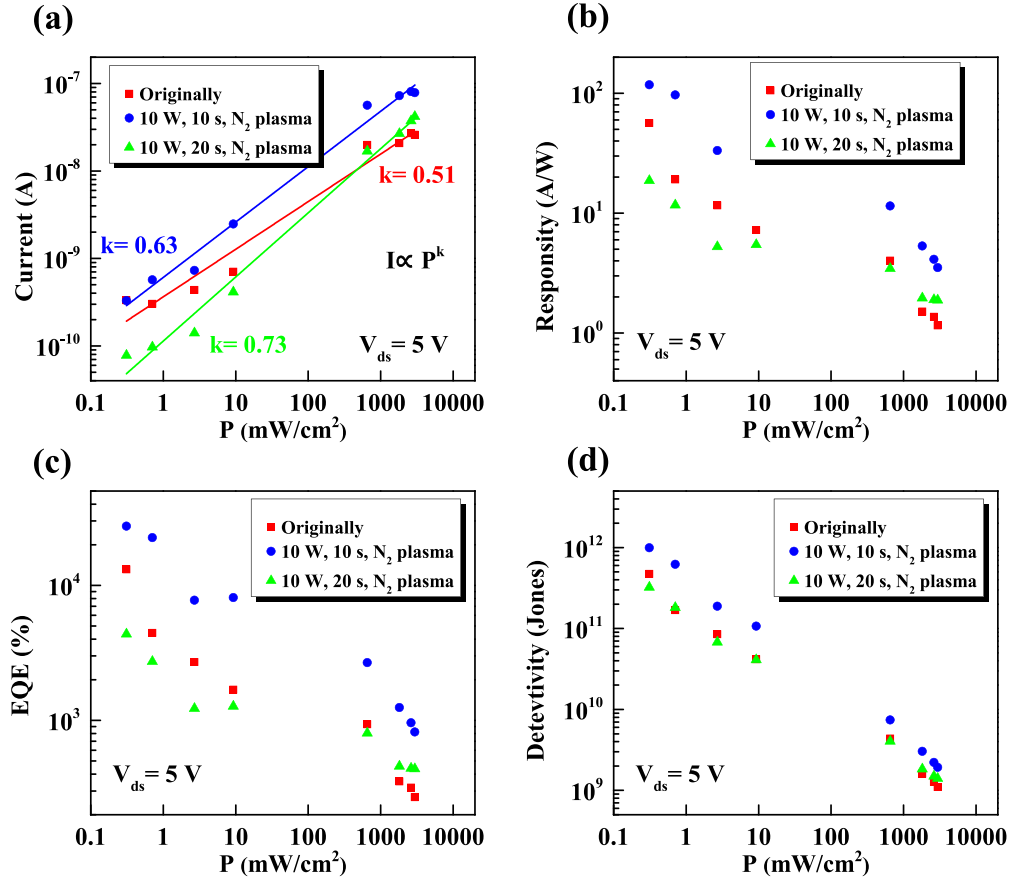
Figure 5. (a) Dependence between light current and power intensity of the single GaAs NW photodetector before and after nitrogen plasma treatment; (b) dependence between responsivity and power intensity of the single GaAs NW photodetector before and after nitrogen plasma treatment; (c) dependence between EQE and power intensity of the single GaAs NW photodetector before and after nitrogen plasma treatment; (d) dependence between specific detectivity and power intensity of the single GaAs NW photodetector before and after nitrogen plasma treatment.

where h is the Planck constant, c is the speed of light, e is the electron charge, λ is the wavelength of the incident light.

The specific detectivity (D^*) is related to the detection sensitivity of a photodetector, which indicates the ability of a photodetector to detect weak signal, and is one of the important parameters to measure the performance of photodetectors. The specific detectivity can be defined as follows [44–46]:

$$D^* = \frac{R}{\sqrt{2e \times I_{\text{dark}}/A}}. \tag{3}$$

The responsivity, EQE and specific detectivity of the single GaAs NW photodetector before and after nitrogen plasma treatment are calculated, and the dependence between the responsivity, EQE, specific detectivity and light power intensity are performed in figures 5(b)–(d). When the light intensity is 0.3 mW cm^{-2}, the responsivity of the nitrogen plasma-treated GaAs device exhibits a significant change in performance. Before treatment, the responsivity is about 56.4 A W^{-1}. After nitrogen plasma treatment, the responsivity increases first, reaching to 117.6 A W^{-1}, which is better than the commercial GaAs photodetectors and some GaAs-based NW photodetectors [3, 28, 47, 48]. Further increases the treatment

time, the responsivity decreases to 18.7 A W^{-1}. This improvement is further underscored by EQE and specific detectivity metrics. When the light intensity is 2966.8 mW cm^{-2}, the responsivity, EQE and specific detectivity show the similar trends, as summarized in table 1. Nitrogen plasma treatment has improved the performance of GaAs NW photodetector. After nitrogen plasma treatment, the surface states of GaAs NW is passivated, thus the photo-generated carriers trapped by surface states will decrease. The optoelectronic conversion process of photodetectors mainly involves the generation, separation, transport and extraction of photo-generated carriers. The number of photo-generated carriers trapped by surface states decreases, more photo-generated carriers are separated and then transported to the electrodes. The photo-generated carriers are collected by the electrodes and contributed to the light current. Thus, the photodetection performance are enhanced after nitrogen plasma treatment.

The different changes in the performance of GaAs NW photodetector under low light intensity and high light intensity may be related to the following reasons: nitrogen plasma treatment can improve the quality of NWs, but when the plasma treatment time is prolonged, the quality of the interface may decrease. At low incident power, more photo-generated

Table 1. The key performance of the GaAs NW photodetector before and after nitrogen plasma treatment.

Treatment performance	Power intensity	Originally	10 W, 10 s, N_2 plasma	10 W, 20 s, N_2 plasma
R (A W^{-1})	0.3 mW cm^{-2}	56.4	117.6	18.7
	2966.8 mW cm^{-2}	1.2	3.5	1.9
EQE (%)	0.3 mW cm^{-2}	13 146	27 434	4359
	2966.8 mW cm^{-2}	270	821	438
D^* (Jones)	0.3 mW cm^{-2}	4.7×10^{11}	9.9×10^{11}	3.2×10^{11}
	2966.8 mW cm^{-2}	1.1×10^9	1.9×10^9	1.4×10^9
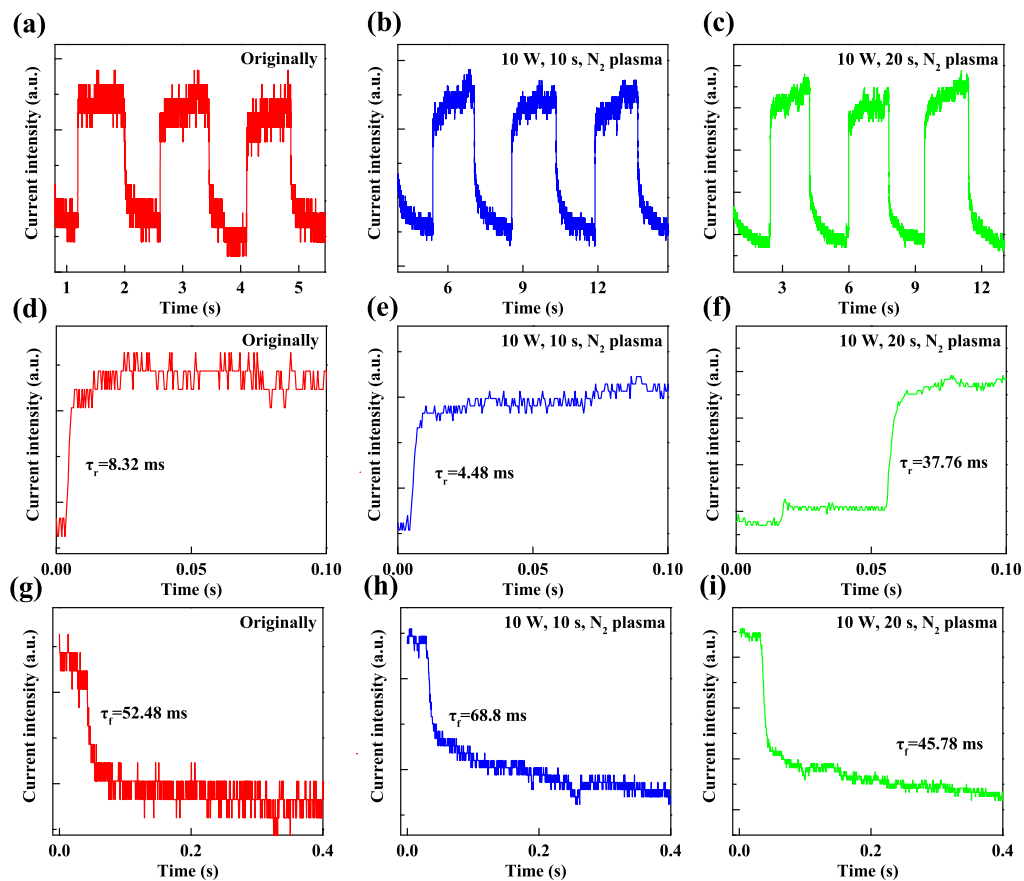
Figure 6. (a) The response time of the original GaAs NW photodetector; (b) the response time of the GaAs NW photodetector after nitrogen plasma treatment for 10 s; (c) the response time of the GaAs NW photodetector after nitrogen plasma treatment for 20 s; (d) the rise time of the original GaAs NW photodetector; (e) the rise time of the GaAs NW photodetector after nitrogen plasma treatment for 10 s; (f) the rise time of the GaAs NW photodetector after nitrogen plasma treatment for 20 s; (g) the fall time of the original GaAs NW photodetector; (h) the fall time of the GaAs NW photodetector after nitrogen plasma treatment for 10 s; (i) the fall time of the GaAs NW photodetector after nitrogen plasma treatment for 20 s.

carriers are captured by interface defects, leading to a decrease in device performance. However, at high incident power, although part of the photo-generated carriers will be captured by interface defects, resulting in a decrease in device performance, some other photo-generated carriers will excited by high energy incident to produce photocurrent. This is consistent with the change of the device performance.

Response time is another important parameter of a photodetector, which characterizes the speed of a photodetector to sense optical signal. Response time includes rise time (τ_r)

and fall time (τ_f), the rise time is defined as the time for the net photocurrent rises from 10% to 90% and the fall time is defined as the time for the net photocurrent fall from 90% to 10%. The response time of the single GaAs NW photodetector before and after nitrogen plasma treatment are shown in figure 6. As shown in figures 6(a)–(c), the GaAs NW photodetectors before and after nitrogen plasma treatments show stable photoresponse. Figures 6(d)–(i) show the detailed rise time and fall time of the devices. After nitrogen plasma treatment, the photocurrent rise time change from 8.32 ms to 4.48 ms and

37.76 ms, the photocurrent fall time change from 52.48 ms to 68.8 ms and 45.78 ms. The change in the photoresponse time also related to the change in the defect states before and after nitrogen plasma treatment.

5. Conclusion

In this work, the effect of nitrogen plasma treatment on the performance of GaAs NW photodetector is investigated. The results show that the light current, responsivity, specific detectivity and EQE of GaAs NW photodetector are obviously improved. Besides, the response times of the photodetectors are also studied. After nitrogen plasma treatment with proper treatment time, the photoresponse rise time decreases, and the photoresponse fall time increases. These results are related to the change of defect states density after nitrogen plasma treatment. This work has promoted the further development of GaAs NW photodetectors and will further promote their application in both civilian and military fields, especially in the field of biological detection.

Data availability statement

All data that support the findings of this study are included within the article (and any supplementary files).

ORCID iDs

Hao Huang ⬛ https://orcid.org/0000-0003-0456-3962
Dong Xu ⬛ https://orcid.org/0000-0002-4559-0775
Shuo Li ⬛ https://orcid.org/0000-0001-8764-5116

References

[1] Konstantatos G, Clifford J, Levina L and Sargent E H 2007 Sensitive solution-processed visible-wavelength photodetectors *Nat. Photon.* **1** 531
[2] Levine B F 1993 Quantum-well infrared photodetectors *J. Appl. Phys.* **74** R1
[3] Peumans P, Yakimov A and Forrest S R 2003 Small molecular weight organic thin-film photodetectors and solar cells *J. Appl. Phys.* **93** 3693
[4] Yan W, Mechau N, Hahn H and Krupke R 2010 Ultraviolet photodetector arrays assembled by dielectrophoresis of ZnO nanoparticles *Nanotechnology* **21** 115501
[5] Park E-S, Jang D-H, Lee Y-I, Jung C W, Lim D W, Kim B S, Jeong Y-K, Myung N V and Choa Y-H 2014 Fabrication and sensing property for conducting polymer nanowire-based biosensor for detection of immunoglobulin G *Res. Chem. Intermed.* **40** 2565
[6] Phuruangrat A, Ekthammathat N, Thongtem S and Thongtem S 2013 Preparation of LaPO$_4$ nanowires with high aspect ratio by a facile hydrothermal method and their photoluminescence *Res. Chem. Intermed.* **39** 1363
[7] Patolsky F, Zheng G, Hayden O, Lakadamyali M, Zhuang X and Lieber C M 2004 Electrical detection of single viruses *Proc. Natl Acad. Sci. USA* **101** 14017
[8] Hahm J-I and Lieber C M 2004 Direct ultrasensitive electrical detection of DNA and DNA sequence variations using nanowire nanosensors *Nano Lett.* **4** 51
[9] Heller A and Feldman B 2008 Electrochemical glucose sensors and their applications in diabetes management *Chem. Rev.* **108** 2482
[10] Du X, Li Y, Motley J R, Stickle W F and Herman G S 2016 Glucose sensing using functionalized amorphous In-Ga-Zn-O field-effect transistors *ACS Appl. Mater. Interfaces* **8** 7631
[11] Rees F, Hui M and Doherty M 2014 Optimizing current treatment of gout *Nat. Rev. Rheumatol.* **10** 271
[12] Weintraub A S *et al* 2015 Impact of renal function and protein intake on blood urea nitrogen in preterm infants in the first 3 weeks of life *J. Perinatol.* **35** 52
[13] Sirbuly D J, Tao A, Law M, Fan R and Yang P 2007 Multifunctional nanowire evanescent wave optical sensors *Adv. Mater.* **19** 61
[14] Minot E D, Kelkensberg F, van Kouwen M, van Dam J A, Kouwenhoven L P, Zwiller V, Borgström M T, Wunnicke O, Verheijen M A and Bakkers E P A M 2007 Single quantum dot nanowire LEDs *Nano Lett.* **7** 367
[15] Dong Y, Tian B, Kempa T J and Lieber C M 2009 Coaxial group III−nitride nanowire photovoltaics *Nano Lett.* **9** 2183
[16] Boland J L, Casadei A, Tutuncuoglu G, Matteini F, Davies C L, Jabeen F, Joyce H J, Herz L M, Fontcuberta I Morral A and Johnston M B 2016 Increased photoconductivity lifetime in GaAs nanowires by controlled n-type and p-type doping *ACS Nano* **10** 4219
[17] Dai X, Zhang S, Wang Z, Adamo G, Liu H, Huang Y, Couteau C and Soci C 2014 GaAs/AlGaAs nanowire photodetector *Nano Lett.* **14** 2688
[18] Kang Y, Hou X, Zhang Z, Meng B, Tang J, Hao Q and Wei Z 2025 Enhanced visible-NIR dual-band performance of GaAs nanowire photodetectors through phase manipulation *Adv. Opt. Mater.* 2500289
[19] Kang Y, Hou X, Zhang Z, Tang J, Lin F, Li K, Hao Q and Wei Z 2024 Ultrahigh-performance and broadband photodetector from visible to shortwave infrared band based on GaAsSb nanowires *Chem. Eng. J.* **501** 157392
[20] Shang F *et al* 2024 Effective surface passivation of GaAs nanowire photodetectors by a thin ZnO capping *Nanoscale* **16** 12534
[21] Dufouleur J, Colombo C, Garma T, Ketterer B, Uccelli E, Nicotra M and Fontcuberta I Morral A 2010 P-doping mechanisms in catalyst-free gallium arsenide nanowires *Nano Lett.* **10** 1734
[22] Sandroff C J, Nottenburg R N, Bischoff J C and Bhat R 1987 Dramatic enhancement in the gain of a GaAs/AlGaAs heterostructure bipolar transistor by surface chemical passivation *Appl. Phys. Lett.* **51** 33
[23] Zhang X, Li A Z, Lin C, Zheng Y L, Xu G Y, Qi M and Zhang Y G 2003 The effects of (NH$_4$)$_2$S passivation

treatments on the dark current–voltage characteristics of InGaAsSb PIN detectors *J. Cryst. Growth* **251** 782

[24] Ravi M R, DasGupta A and DasGupta N 2003 Effect of sulfur passivation and polyimide capping on InGaAs-InP PIN photodetectors *IEEE Trans. Electron Devices* **50** 532

[25] Alekseev P A, Dunaevskiy M S, Ulin V P, Lvova T V, Filatov D O, Nezhdanov A V, Mashin A I and Berkovits V L 2015 Nitride surface passivation of GaAs nanowires: impact on surface state density *Nano Lett.* **15** 63

[26] Dhindsa N, Chia A, Boulanger J, Khodadad I, LaPierre R and Saini S S 2014 Highly ordered vertical GaAs nanowire arrays with dry etching and their optical properties *Nanotechnology* **25** 305303

[27] Tajik N *et al* 2011 Sulfur passivation and contact methods for GaAs nanowire solar cells *Nanotechnology* **22** 225402

[28] Chen X, Xia N, Yang Z, Gong F, Wei Z, Wang D, Tang J, Fang X, Fang D and Liao L 2018 Analysis of the influence and mechanism of sulfur passivation on the dark current of a single GaAs nanowire photodetector *Nanotechnology* **29** 095201

[29] Salihoglu O, Muti A and Aydinli A 2013 A comparative passivation study for InAs/GaSb pin superlattice photodetectors *IEEE J. Quantum Electron.* **49** 661

[30] Chang C-C *et al* 2012 Electrical and optical characterization of surface passivation in GaAs nanowires *Nano Lett.* **12** 4484

[31] Chia A C E, Tirado M, Li Y, Zhao S, Mi Z, Comedi D and LaPierre R R 2012 Electrical transport and optical model of GaAs-AlInP core-shell nanowires *J. Appl. Phys.* **111** 094319

[32] Guo S, Yang D, Wang D, Fang X, Fang D, Chu X, Yang X, Tang J, Liao L and Wei Z 2022 Response improvement of GaAs two-dimensional non-layered sheet photodetector through sulfur passivation and plasma treatment *Vacuum* **197** 110792

[33] Irish A, Zou X, Barrigon E, D'Acunto G, Timm R, Borgström M T and Yartsev A 2022 Nitrogen plasma passivation of GaAs nanowires resolved by temperature dependent photoluminescence *Nano Express* **3** 045008

[34] André Y *et al* 2020 Optical and structural analysis of ultra-long GaAs nanowires after nitrogen-plasma passivation *Nano Express* **1** 020019

[35] Chen X *et al* 2019 Enhanced photoresponsivity of a GaAs nanowire metal-semiconductor-metal photodetector by adjusting the Fermi level *ACS Appl. Mater. Interfaces* **11** 33188

[36] Zhang L *et al* 2016 Self-catalyzed molecular beam epitaxy growth and their optoelectronic properties of vertical GaAs nanowires on Si(111) *Mater. Sci. Semicond. Process.* **52** 68

[37] Cao Y L *et al* 2011 Single-crystalline ZnTe nanowires for application as high-performance green/ultraviolet photodetector *Opt. Express* **19** 6100

[38] Luo L, Chen J, Wang M, Hu H, Wu C-Y, Li Q, Wang L, Huang J-A and Liang F-X 2014 Near-infrared light photovoltaic detector based on GaAs nanocone array/monolayer graphene Schottky junction *Adv. Funct. Mater.* **24** 2794

[39] Zheng D *et al* 2018 High-performance near-infrared photodetectors based on p-type SnX (X= S, Se) nanowires grown via chemical vapor deposition *ACS Nano* **12** 7239–45

[40] Luo T, Liang B, Liu Z, Xie X, Lou Z and Shen G 2015 Single-GaSb-nanowire-based room temperature photodetectors with broad spectral response *Sci. Bull.* **60** 101

[41] Gong F, Wu F, Long M, Chen F, Su M, Yang Z and Shi J 2018 Black phosphorus infrared photodetectors with fast response and high photoresponsivity *Phys. Status Solidi* **12** 1800310

[42] Yang Z, Liao L, Gong F, Wang F, Wang Z, Liu X, Xiao X, Hu W, He J and Duan X 2018 WSe$_2$/GeSe heterojunction photodiode with giant gate tunability *Nano Energy* **49** 103

[43] Smilyk V O, Fomanyuk S S, Kolbasov G Y, Rusetskyi I A and Vorobets V S 2019 Electrodeposition, optical and photoelectrochemical properties of BiVO$_4$ and BiVO$_4$/WO$_3$ films *Res. Chem. Intermed.* **45** 4149

[44] Zhang X, Liu Q, Liu B, Yang W, Li J, Niu P and Jiang X 2017 Giant UV photoresponse of a GaN nanowire photodetector through effective Pt nanoparticle coupling *J. Mater. Chem. C* **5** 4319

[45] Zheng D *et al* 2016 When nanowires meet ultrahigh ferroelectric field-high-performance full-depleted nanowire photodetectors *Nano Lett.* **16** 2548

[46] Gong F *et al* 2016 High-sensitivity floating-gate phototransistors based on WS$_2$ and MoS$_2$ *Adv. Funct. Mater.* **26** 6084

[47] Persson A I, Ohlsson B J, Jeppesen S and Samuelson L 2004 Growth mechanisms for GaAs nanowires grown in CBE *J. Cryst. Growth* **272** 167

[48] Li Z, Yuan X, Fu L, Peng K, Wang F, Fu X, Caroff P, White T P, Hoe Tan H and Jagadish C 2015 Room temperature GaAsSb single nanowire infrared photodetectors *Nanotechnology* **26** 445202